ACCESS REQUIREMENTS FOR STATIONARY ELM-SUPPRESSED PEDESTALS IN DIII-D AND C-MOD H-MODE AND I-MODE PLASMAS

T.M. WILKS, S.G. BAEK, A.E. HUBBARD, J.W. HUGHES
Massachusetts Institute of Technology, Plasma Science and Fusion Center
Cambridge, MA, USA
Email: twilks@psfc.mit.edu

K.K BARADA
University of California Los Angeles
Los Angeles, CA, USA

K.H. BURRELL, XI CHEN, A.M. GAROFALO
General Atomics
San Diego, CA, USA

P.H. DIAMOND
University of California San Diego
San Diego, CA, USA

Z.B. GUO
Peking University
Beijing Shi, China

C.G. THEILER
EPFL
Lausanne, Switzerland

Abstract

Analysis of pedestal characteristics for Quiescent H-mode (QH-mode) and I-mode plasmas from recent experiments on DIII-D and C-Mod investigates the role of the radial electric field and ExB shear and edge fluctuation characteristics that govern pedestal performance and ELM avoidance. In DIII-D standard QH-mode plasmas, critical values of ExB shear are required in experiment to suppress the transition from QH-mode to conventional ELMy H-mode. The experimental shear values exhibit similar trends with predicted scaling parameters from a recent non-linear phase dynamics model linking pressure and velocity perturbations. However, this first theoretical effort over-estimates the order of the magnitude of the critical values measured in experiment. With lower ExB shear, broadband turbulence is observed to emerge in experiment, which appears to regulate pedestal gradients below kinetic ballooning and peeling ballooning stability thresholds and is sometimes associated with a pedestal that grows higher and wider than a standard pedestal governed by these physics limitations. On DIII-D, these transport limited pedestals can lead to Wide Pedestal QH-modes (WPQH) and on C-Mod, the I-mode can be accessed, which lacks an edge particle transport barrier. On DIII-D, the WPQH is subject to a limit cycle behavior with increasing frequency and amplitude of density fluctuations as shaping is reduced, with turbulent fluctuations across the pedestal in ion and electron channels. The maximum achievable radial electric field well in I-mode increases with magnetic field strength, suggesting that optimizing the radial electric field may be important for maintaining access to the I-mode regime, which has a radial electric field typically intermediate to L-modes and H-modes. Different mechanisms can underpin these high performance naturally ELM suppressed scenarios, with access conditions depending on the interaction between the radial electric field, associated ExB shear and turbulence characteristics.

1. INTRODUCTION

H-mode levels of energy confinement are required for the mission of ITER and future reactors. However, the presence of edge localized modes (ELMs) represents a key challenge [1-2]. The periodic bombardment of heat and particles to the wall and divertor from ELMs cannot be tolerated by existing materials, and therefore significant effort is being invested into developing regimes that are intrinsically stable to ELMs [3-4]. Quiescent H-mode (QH-mode) [5-13] and I-mode [14-19] plasmas are two such regimes, which leverage a variety of edge

fluctuations that may relax the pressure gradient in the pedestal by inducing particle transport, allowing operation below the peeling-ballooning stability limit, which governs the onset of ELMs [20].

The characterization of edge fluctuations and sensitivity to common edge turbulence drivers or suppressors such as ExB shear is important for understanding how to leverage the desired edge modes to maintain a stationary pedestal without ELMs. Local and global access conditions to access and maintain 1) standard QH-modes, 2) wide pedestal QH-modes (WPQH), and 3) I-mode regimes will be discussed. Standard QH-mode exists at high ExB shear conditions and exhibits a saturated edge peeling driven mode called the edge harmonic oscillation (EHO), which provides particle transport necessary to remain ELM-free, and has a well-defined pedestal for both temperature and density. The WPQH-mode is intrinsically stable to ELMs via transport provided by increased broadband fluctuations ranging from 1-10^3kHz, and sometimes exhibits a unique limit cycle oscillation (LCO) regime [21] between the density and ExB velocity perturbations. The WPQH has a pedestal in both temperature and density profiles, and forms a pressure pedestal that is higher and wider than is predicted by theory constrained by kinetic ballooning and peeling-ballooning physics [22-23]. I-mode regimes are characterized by a separation of particle and energy transport channels by exhibiting a temperature pedestal, but no density pedestal. The relaxed pressure gradient in I-mode allows ELM-suppressed operation due to particle transport, which is thought to be at least partly due to the edge localized weakly coherent mode (WCM) at 150-300kHz, coupled with a lower frequency fluctuation consistent with being a geodesic acoustic mode (GAM) [24-26].

The standard QH-mode and WPQH were discovered in similar operational regimes on DIII-D and therefore are normally compared directly; the I-mode regime is typically presented as a separate scenario. This discussion aims to make direct comparisons of the WPQH and I-mode regimes, illustrating the similarity of interacting edge fluctuations that generate sufficient transport for the pedestals to not be limited by kinetic ballooning and peeling-ballooning physics. Additionally, further characterization of edge fluctuations, specifically the radial localization and effects on shaping, are discussed, which lays the foundation for comparison to simulations and performance optimization of each scenario in the future.

The radial electric field as associated ExB shear are important parameters for determining access to each regimes. When compared to other regimes as in Fig. 1, the I-mode radial electric field is similar to EDA H-mode plasmas obtained with favourable grad-B drift, which is another stationary ELM-free regime primarily studied in C-Mod, and ranges from 30-110kV/m. The I-mode and EDA H-mode Er wells are consistently smaller than ELMy H-modes and transient ELM-free H-modes which typically range between 100-300 kV/m, and are larger than the Er wells in L-mode which are closer to 30 kV/m.

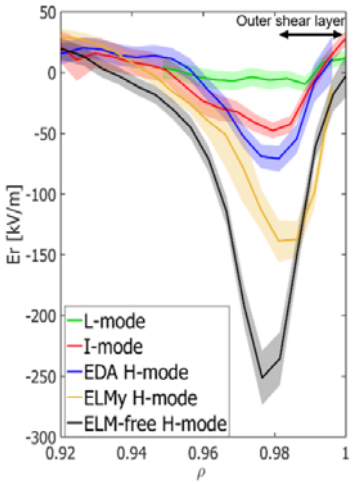

FIG. 1. *Radial electric fields compared across regimes for some typical C-Mod plasmas. As discussed later, the Er well can have a wide variation with parameters such as magnetic field and input power*

.

Understanding how to access and maintain naturally ELM suppressed pedestals requires characterization of edge turbulence mechanisms, a high level perspective for comparing and contrasting regimes, as well as a detailed understanding of sensitivity to important turbulence driving and damping mechanisms like the radial electric field and ExB shear. The edge turbulence, pedestal profiles, and experimental access conditions for these naturally ELM free plasmas are beginning to be understood, but further studies are required to understand the physical

drivers and theoretical understanding of these edge turbulent and MHD modes in order to leverage and control them.

2. CHARACTERIZATION OF PEDESTAL TURBULENCE IN NATURALLY ELM FREE REGIMES: STANDARD QH-MODE, WIDE PEDESTAL QH-MODE, AND I-MODE

Full characterization of the fluctuation mechanisms is being mapped out for different pedestal regimes. Understanding the drivers and subsequent transport associated with each fluctuation is essential for optimized control in the future. Previous research has characterized the pedestal modes in standard QH-mode [27-28] and WPQH regimes [22-23,29] in DIII-D and I-modes [19,30-33] in primarily C-Mod plasmas, but also some in DIII-D [34]. Table 1 compares the dominant modes observed in the three ELM-free regimes, their diamagnetic direction, and radial localization.

TABLE 1. COMPARISON OF ELM FREE PEDESTAL MODE CHARACTERISTICS

Regime	Dominant Features	Diamagnetic Direction	Radial Location
Standard QH-mode	1) EHO 2) Broadband	1) Electron 2) Electron	1) Entire Pedestal 2) Entire Pedestal
WPQH	1) Broadband 2) Broadband 3) Broadband	1) Ion 2) Electron 3) Electron	1) Entire Pedestal 2) Middle of Er well 3) Pedestal top
I-mode	1) WCM 2) GAM	1) Electron 2) None	1) Outer Er shear layer 2) Outer Er shear layer

The standard QH-mode has one very dominant feature, the EHO, which exists in conjunction with background broadband turbulence. However, the WPQH and the I-mode have two or more distinct branches of turbulence. In the case of the I-mode, it has been shown that energy transfer between the WCM and the GAM allow a broadened frequency spectrum of the WCM. The WPQH has a plethora of identified edge turbulent modes that have been measured, though interaction between them is yet to be shown. The WPQH can exist with either 1) broadband MHD and an EHO, or 2) broadband MHD and a limit cycle oscillation (LCO). The LCO is a stationary regime characterized by a predator-prey relationship between the density fluctuations and the ExB velocity [21]. Table 2 summarizes more of the turbulence characteristics between the ELM-free regimes, highlighting the complexity of potential drivers of particle transport able to be leveraged as gradient relaxation mechanisms. These exist at a wide range of frequencies, wave numbers, radial locations in the pedestal, and toroidal mode numbers.

TABLE 2. COMPARISON OF ELM FREE PEDESTAL FLUCTUATION CHARACTERISTICS

Regime	Dominant Features	Frequency	n	k_θ [cm^{-1}]
Standard QH-mode	1) EHO 2) Broadband	1) 5-40kHz 2) 100-500 kHz	1) 1-5 2) Unknown	1) 0.02-0.2 2) 0.5-1.5
WPQH	1) Broadband 2) Broadband 3) Broadband	1) 10-100kHz 2) 500-800 kHz 3) > 800 kHz	1) Many 2) Many 3) Unknown	1) ~0.1 2) ~4-6 3) Unknown
I-mode	1) WCM 2) GAM	1) 150-300 kHz 2) 10-30 kHz	1) 20 2) 0	1) ~2 2) ~0-1

To further characterize the I-mode pedestal, the reflectometer analysis shown in Fig. 2 for C-Mod I-mode plasmas radially localizes density fluctuations associated with the WCM and GAM frequencies in the outer shear layer of the Er well and extending out to the separatrix. Previous studies using the gas puff imaging system on C-Mod [32] are in agreement with this analysis, though they also show cases of these modes extending further into the pedestal. In Fig. 2, the WCM feature is present on both the 88GHz and 75GHz reflectometer frequencies, which span the

steep gradient region of the electron temperature pedestal. The low frequency GAM feature is only present on the 75GHz reflectometer channel near the foot of the electron density pedestal for the discharge shown, providing the potential to expel particles from the confined plasma into the scrape off layer.

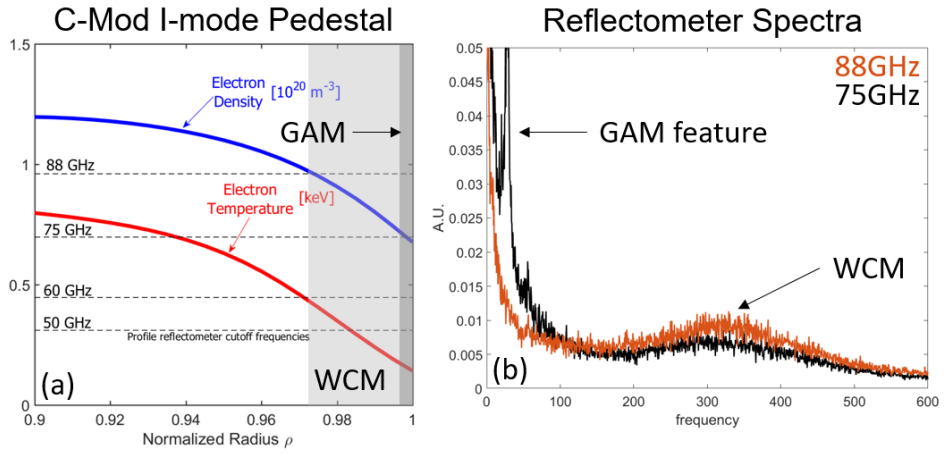

FIG 2: *a) Density and temperature pedestal of a C-Mod I-mode with radial localization of the WCM and GAM frequency density fluctuations using reflectometry. b) Reflectometer power spectra at 88GHz and 75GHz frequencies showing the WCM and GAM features in frequency space.*

The WPQH has a unique limit cycle oscillation that is sensitive to plasma triangularity. Doppler backscattering measurements in DIII-D show plasma shape affects both density fluctuations and frequency of the LCO, as shown in Fig. 3. The ITER-like shape exhibits larger density fluctuations by almost an order of magnitude and a higher LCO frequency than the double null (DN) shape as in Fig. 3b. The smaller magnitude fluctuations are associated with a larger triangularity for the DN shape ($\delta_u^{DN} = 0.65$) as compared to the ITER-like shape ($\delta_u^{DN} = 0.35$). The larger density fluctuation in the ITER-like shape elongates the phase space of the LCO defined by the Doppler velocity and the density fluctuation, though the two shapes span very similar ranges in Doppler velocity magnitude as shown in Fig. 3a. It has previously been reported that the LCO frequency is inversely proportional to plasma density, which is in agreement with this finding [21].

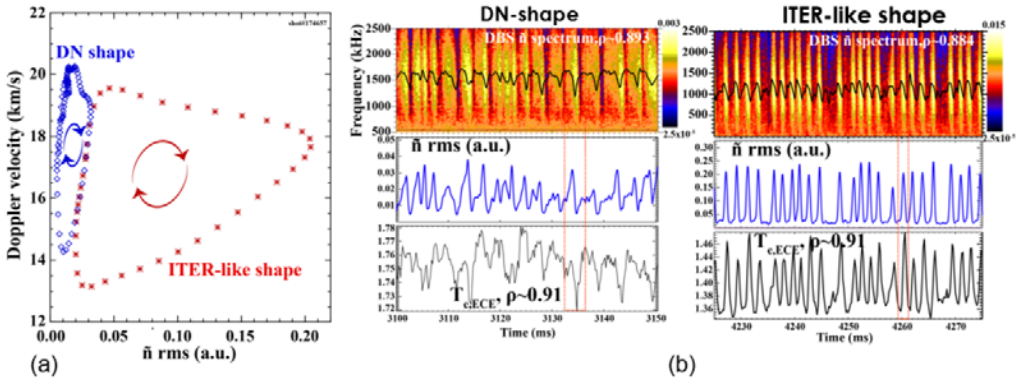

FIG. 3. *a) The LCO present at the top of the pedestal in WPQH plasmas is elongated in phase space with decreased plasma shaping b) Lower triangularity associated with the elongated LCO phase space has higher frequency and amplitude density fluctuations measured by Doppler backscattering than the higher triangularity double null shape.*

Triangularity is a key parameter in defining the extent of the peeling-ballooning stability boundary, as shown in Fig. 4 for example, by codes such as ELITE [35]. Typical experimental operating points for WPQH and I-mode lie in the stable region [19,22], indicating another driver for edge pedestal MHD and turbulent activity which provides particle transport to maintain an ELM-free pedestal beyond peeling-ballooning physics. The EHO in the standard QH-mode is thought to be a saturated kink-peeling mode. Even though both the standard QH-mode and the wide pedestal QH-mode share a similar name, the turbulence and MHD stability characteristics allowing the

two regimes to remain ELM-free appear to be different, and even suggest more of a similarity between I-mode and WPQH.

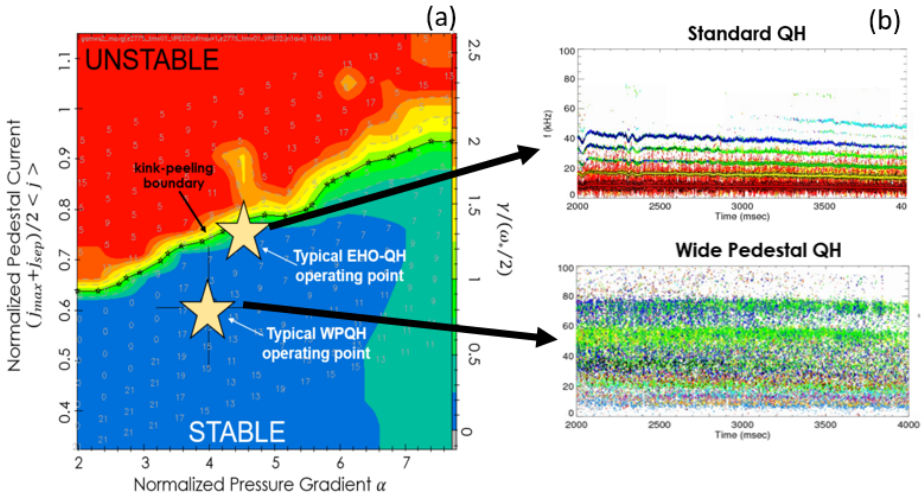

FIG 4: *a) Contour plot of the ratio of the growth rate of the dominant mode calculated by ELITE to half of the ion diamagnetic frequency, ω_*, where the horizontal axis is the normalized peak pressure gradient and the vertical axis is the ratio of the average pedestal current to volume averaged current density b) Frequency spectra for the edge harmonic oscillation typically observed in standard QH-modes which usually operate at the kink/peeling boundary versus broadband MHD typically seen in WPQH-mode plasmas which usually operate below the kink/peeling boundary.*

Both the WPQH and the I-mode are stable to peeling-ballooning and kinetic ballooning limits as shown in Fig. 5, and exhibit pedestals that are wider than EPED would predict for a pedestal limited by PB/KBM physics with the same pressure at the pedestal top. In DIII-D the WPQH regime derives its name from having a higher and wider pedestal than EPED predicts for standard H-mode pedestals under similar conditions, and I-modes in DIII-D exhibit similar features as shown by Fig. 5, which is in agreement with previous studies done on C-Mod I-modes [19].

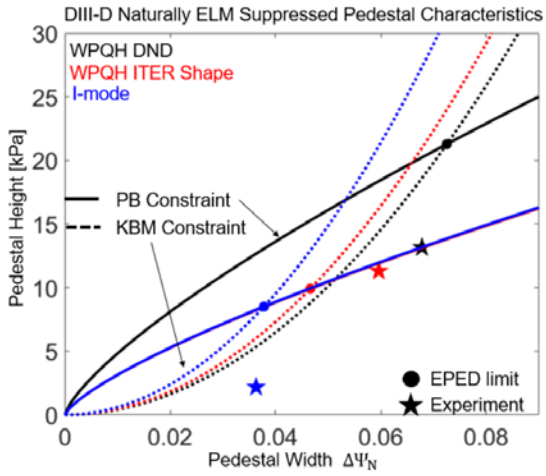

FIG 5: *The experimental pedestal widths for DIII-D I-modes and WPQH-modes exceed that of the EPED prediction for a pedestal with the same height limited by peeling ballooning and kinetic ballooning mode physics. This result agrees with I-modes found in C-Mod plasmas [19].*

3. ACCESS CONDITIONS FOR SUSTAINMENT OF ELM FREE PEDESTALS THROUGH EXB SHEAR

The role of the radial electric field and ExB shear in the pedestal region is important for accessing and remaining in both types of QH-modes as well as I-mode plasmas. There is good evidence experimentally, and it has been predicted theoretically, that there is a critical ExB shearing rate required for the onset of the EHO in standard QH-mode [8,27,36-37]. Experimental studies of the WPQH show broader radial electric field wells and ExB shearing rate profile structures, usually with a smaller peak magnitude in the edge region than a corresponding standard QH-mode. Access to the I-mode window is extended with higher L-H power thresholds, and I-mode usually has an Er well intermediate between an L-mode and a typical H-mode (Fig. 1), indicating that the radial electric field and ExB shear in the edge pedestal affect access conditions to this ELM free regimes.

3.1 DIII-D Quiescent H-mode Plasmas

A nonlinear phase-dynamics model [37] relating the pressure and velocity perturbations in the edge pedestal region predicts the critical ExB shear required for onset of the EHO observed in standard QH-modes. This is the first theory to predict an ExB shearing rate threshold, which is also observed in experiment. The theory predicts a linear relationship between critical shearing rate and $c_s/\sqrt{L_p \Delta x}$, where c_s is the ion acoustic velocity, L_p the pressure gradient scale length, and Δx is the radial width of the mode. When compared to standard DIII-D QH-mode plasmas, the theoretical scaling of the critical shearing rate agrees with experiment, but the absolute magnitude of the limit is over-predicted by the theory by two orders of magnitude. Through a normalized predicted scaling, the model demonstrates the dynamic transition into and out of QH-mode qualitatively within a single plasma discharge, as shown in Fig. 6. The magenta points in Fig. 6b correspond to the discharge shown in Fig. 6a, where the phase space defined by the predicted scaling separates critical ExB shearing rates (shown mostly within the gray shaded uncertainty of the fit to the scaling in Fig. 6b) from those when the plasma is operating in a robust QH-mode. The other points in the scaling correspond to 43 other critical transition points to calculate the scaling trend. Comparison of experiment with the theory lends insight into improving the theoretical model by including more realistic geometry and toroidal mode number physics for more accurate quantitative predictions [36].

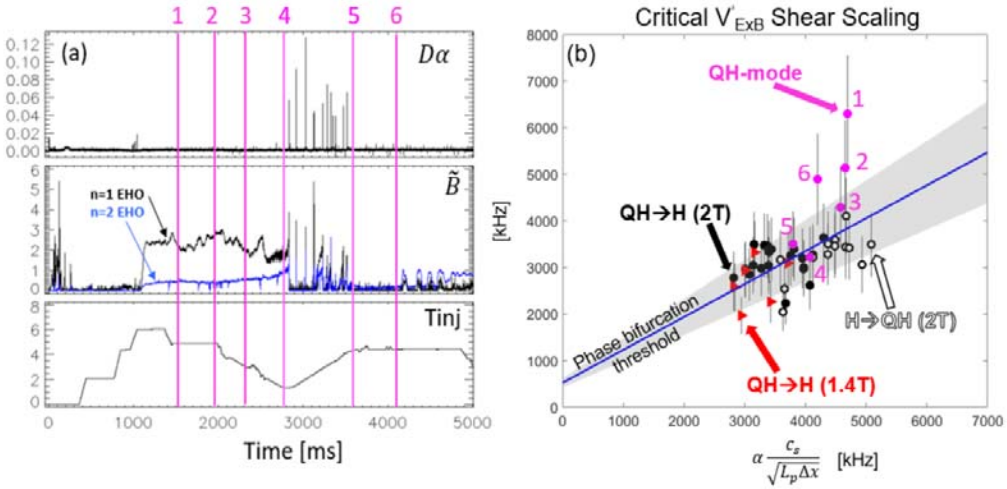

FIG 6. a) Time history of DIII-D discharge #163466 showing the D-alpha trace illustrating the onset of ELMs, the n=1 and n=2 magnetic fluctuations from the Mirnov coils, and injected torque. b) Evolution of the same shot in the phase space defined by critical ExB shear and the Guo-Diamond scaling parameters where the numbered time slices in panel (a) correspond to the points in panel (b) shown in conjunction with data from 43 other experimental critical ExB shearing rates..

3.2 C-Mod I-mode Plasmas

C-Mod I-mode pedestals analyzed over a range magnetic fields (2.8-5.8T) and auxiliary power (1.5-4.6 MW) show consistent edge fluctuation behavior exhibiting both WCM and GAM frequency features [26]. There is a broad range of radial electric field well depths possible for fixed B_ϕ due to varied pressure gradient and intrinsic

rotation conditions, as shown in Fig. 7. There is also a broad range of ExB shear values, especially for the outer Er shear layer with increased magnetic field. The inner shear layer consistently is smaller in magnitude than the outer shear layer, with the upper limit of inner shear corresponding to similar values as the lower limit of the outer shear.

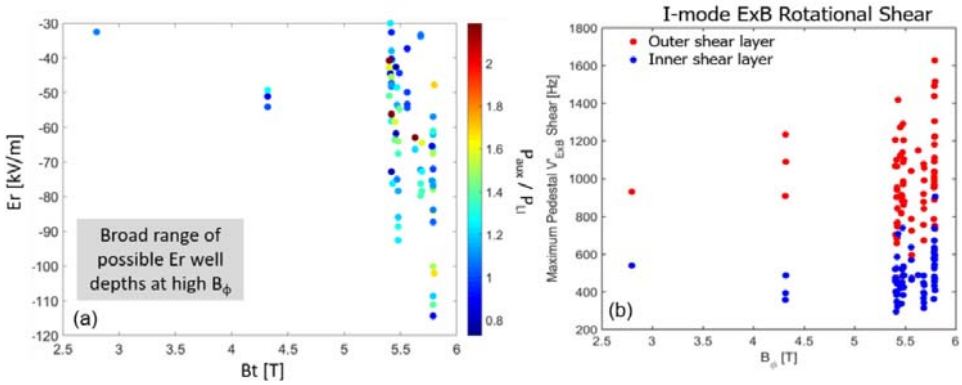

FIG. 7. a) Radial electric field well depths and b) ExB shear for a broad range of C-Mod I-mode discharges. Maximum measured E_r well depth and shear increase with magnetic field.

The maximum possible experimental radial electric field and ExB shear magnitudes increase with toroidal magnetic field. This suggests that the expanded window for I-mode at high field may be linked to a critical value of E_r/B required to induce an H-mode transition, leading to broader access conditions to I-mode in higher magnetic field devices.

4. CONCLUSIONS

Similarities have been identified between the WPQH and I-mode regimes: 1) they both operate below the peeling-ballooning stability boundary outside of error bars indicating an alternative drive for pedestal instabilities, 2) have several unique MHD and/or turbulence features that are separated in frequency space wave number, and 3) their experimentally measured pressure pedestal widths exceed the pressure gradient limit due to the KBM predicted scaling calculated by EPED.

Full characterization of the WPQH and I-mode pedestals is necessary for optimization of the scenarios and understanding the connection of these pedestal fluctuations and transport. Doppler backscattering measurements in DIII-D WPQH-modes localize the LCO to the top of the pedestal, and show that decreased average triangularity extends the LCO phase space and increases both the fluctuation amplitude and frequency, suggesting plasma shape could be used as a parameter for controlling the optimal level of pedestal transport. Further characterization of I-mode pedestals radially localizes the edge fluctuations. Reflectometer measurements in C-Mod I-mode plasmas coupled with Thomson scattering electron pedestal profiles localize the weakly coherent mode and geodesic acoustic mode fluctuations to the outside of the Er well, suggesting control of the Er well depth and location could be important to controlling the interactions between the WCM and the GAM fluctuations.

The radial electric field and ExB shear play an important role in accessing and maintaining each of these regimes. For standard QH-modes, there is a critical ExB shearing rate required for EHO onset both measured in DIII-D experiments and predicted by theory. The theory qualitatively agrees with the parameter scaling from experiment, but over-predicts the critical ExB shearing rate by two orders of magnitude. Through a normalized predicted ExB shear scaling, theory can predict the transition into and out of QH-mode of a standard QH-mode in DIII-D. C-Mod I-modes exhibit consistent turbulence characteristics over a range of magnetic fields from 2.8-5.6T, but lack a scaling with Er quantities, suggesting Er plays a role in terms of global access to I-mode, but may not act as a direct drive or damper on the fluctuations that drive transport, unlike standard QH-modes. There are a broad range of radial electric field wells and ExB shear whose maximum values increase with magnetic field strength. With respect to Er and ExB shear, access to C-Mod I-modes is limited by the transition into H-mode, and an increase in maximum allowable Er well depth with magnetic field indicates a possible critical Er/B value defining the upper limit of the I-mode access window. The I-mode radial electric field in C-Mod plasmas is consistent in magnitude with the other commonly observed ELM-suppressed regime EDA H-mode in the favorable grad-B drift configuration, which is intermediate to ELMing H-modes and L-mode Er well values.

ACKNOWLEDGEMENTS

The efforts of the DIII-D and C-Mod teams were essential to this work and greatly appreciated. This research was supported by the U.S. Department of Energy, Office of Science, and Office of Fusion Energy Sciences using the DIII-D National Fusion Facility under awards DE-FC02-04ER54698 and DE-FG02-04ER54738 and MIT cooperative agreement DE-SC0014264. DIII-D data shown in this paper can be obtained in digital format by following the links at https://fusion.gat.com/global/D3D_DMP.

REFERENCES

[1] T. Eich et. al., Journ. Nucl. Mater. 337-339, 669-676 (2005)
[2] A. Loarte et. al., Journ. Nucl. Mater. 463, 401-405 (2014)
[3] R. Maingi, Nucl. Fusion 54, 114016 (2014)
[4] E. Viezzer, Nucl. Fusion accepted 2018. https://doi.org/10.1088/1741-4326/aac222
[5] K.H. Burrell et. al., PoP 5, 2153 (2001)
[6] K.H. Burrell et. al., PoP 12, 056121 (2005)
[7] A.M. Garofalo et. al., Nucl. Fusion 51, 083018 (2011)
[8] K.H. Burrell et. al., Nucl. Fusion 53, 073038 (2013)
[9] A.M. Garofalo et. al.. Phys. Plasmas 22, 056116 (2015)
[10] W. Suttrop et. al., Nucl. Fusion 45 721 (2005)
[11] Y. Sakamoto et. al., Plasma Phys. Control. Fusion 46, a299 (2004)
[12] N. Oyama et. al., Nucl. Fusion 45, 871 (2005)
[13] E.R. Solano et. al., Phys. Rev. Lett. 104, 185003 (2010)
[14] D. Whyte et. al., Nucl. Fusion 50, 105005 (2010)
[15] A. Marinoni et. al., Nucl. Fusion 55, 093019 (2015)
[16] A.H. Hubbard et. al., Nucl. Fusion 57,126039 (2017)
[17] F. Ryter et. al., Nucl. Fusion 57, 016004 (2017)
[18] A.E. Hubbard et. al., Nucl. Fusion 52, 114009 (2012)
[19] J.R. Walk et. al. Phys. of Plasmas 21, 056103 (2014)
[20] P.B. Snyder et. al., Nucl. Fusion 44, 320 (2004)
[21] K. Barada et. al., Phys. Rev. Lett. 120, 135002 (2018)
[22] Xi Chen et. al., Nucl. Fusion 57, 022007 (2017)
[23] Xi Chen et. al., Nucl. Fusion 57, 086008 (2017)
[24] P. Manz et. al., Nucl. Fusion 55, 083004 (2015)
[25] I. Cziegler et. al., Phys. Rev. Lett. 118, 105003 (2017)
[26] I. Cziegler et. al., Phys. of Plasmas 20, 055904 (2013)
[27] Xi Chen et. al., Nucl. Fusion 56 076011(2016)
[28] J.C Rost et. al., Phys. Plasmas 21, 062306 (2014)
[29] J.C. Rost et. al, Transport Taskforce 2018.
[30] Z.X. Liu et. al., Phys. Plasmas 23, 120703 (2016)
[31] J.W. Hughes et. al., Nucl. Fusion 53 043016 (2013)
[32] C Theiler et. al., Plasma Phys. Control. Fusion 59 025016 (2017)
[33] A. Dominguez. PhD Thesis. Study of density fluctuations and particle transport at the edge of I-Mode plasmas in Alcator C-Mod" (2012).
[34] A. Marinoni et. al., Nucl. Fusion 55 (2015) 093019
[35] P.B. Snyder et. al., Nucl. Fusion 44, 320 (2004)
[36] T.M. Wilks et. al., Nucl. Fusion accepted 2018. https://doi.org/10.1088/1741-4326/aad143
[37] Z.B. Guo and P.H. Diamond, Phys. Rev. Lett. 114, 145002 (2015)